Conjugated Porphyrin Dimers: Cooperative Effects and Electronic Communication in Supramolecular Ensembles with C_{60}

Luis Moreira,[†,ǂ] Joaquín Calbo,[‡] Juan Aragó,[‡] Beatriz M. Illescas,[ǂ] Iwona Nierengarten,[†] Béatrice Delavaux-Nicot,[§] Enrique Ortí,*[,‡] Nazario Martín,*[,ǂ,⊥] and Jean-François Nierengarten.*[,†]

[†] Laboratorie de Chimie des Matériaux Moléculaires. Université de Strasbourg et CNRS (UMR 7509), ECPM, 67087 Strasbourg, Cedex 2, France.

[‡] Instituto de Ciencia Molecular, Universidad de Valencia, 46890 Paterna, Spain.

[ǂ]Departamento de Química Orgánica, Facultad de Ciencias Químicas, Universidad Complutense de Madrid, 28040 Madrid, Spain.

[§] Laboratoire de Chimie de Coordination du CNRS (UPR 8241), Université de Toulouse (UPS, INPT), 31077 Toulouse, Cedex 4, France.

[⊥] Imdea-Nanoscience, Campus Cantoblanco, 28049 Madrid (Spain).

KEYWORDS fullerene receptors, porphyrins, crown ethers, supramolecular chemistry, molecular modeling.

ABSTRACT: Two new conjugated porphyrin-based systems (dimers **3** and **4**) endowed with suitable crown ethers have been synthesized as receptors for a fullerene-ammonium salt derivative (**1**). Association constants in solution have been determined by UV-vis titration experiments in CH_2Cl_2 at room temperature. The designed hosts are able to associate up to two fullerene-based guest molecules and present association constants as high as $\sim 5 \times 10^8$ M^{-1}. Calculation of the allosteric cooperative factor α for supramolecular complexes **[3·1₂]** and **[4·1₂]** showed a negative cooperative effect in both cases. The interactions accounting for the formation of the associates are based, firstly, on the complementary ammonium-crown ether interaction and, secondly, on the π–π interactions between the porphyrin rings and the C_{60} moieties. Theoretical calculations have evidenced a significant decrease of the electron density in the porphyrin dimers **3** and **4** upon complexation of the first C_{60} molecule, in good agreement with the negative cooperativity found in these systems. This negative effect is partially compensated by the stabilizing C_{60}-C_{60} interactions that take place in the more stable *syn*-disposition of **[4·1₂]**.

INTRODUCTION

In recent years, a large variety of porphyrin-fullerene dyads has been studied in the search for efficient charge- and energy-transfer processes of interest in the area of artificial photosynthesis and organic photovoltaics.[1] Although greater efforts have been devoted to the study of covalent hybrids, supramolecular approaches have also been developed. Thus, supramolecular porphyrin-fullerene associates have been built up by π-π interactions,[2] in particular with porphyrin tweezers and cages,[3] metal-ligand bonds,[4] hydrogen bonds,[5] electrostatic interactions,[6] mechanical bonds,[7] or a combination of several of these interactions.[8] Supramolecular arrays involving conjugated multiporphyrin systems are, however, scarce in the literature. Some of us have studied different conjugated polytopic porphyrin receptors with two up to 10 porphyrin subunits.[9] In those systems, a positive cooperative supramolecular effect was encountered and rationalized by the existence of favorable π-π interactions between the different fullerene moieties interacting with the porphyrin rings. However, in such systems the porphyrin subunits behaved independently, as demonstrated by comparison of the absorption and emission spectra of the polytopic receptors with those of the corresponding monotopic porphyrin system. On the other hand, Tashiro and Aida studied the supramolecular interaction of a cyclic receptor formed by two fused porphyrin dimers and C_{60}.[10] This receptor was able to complex one unit of C_{60}, while the introduction of a second fullerene moiety was hindered by a strong negative cooperative effect. In this case, the electronic communication between the two fused porphyrins causes a decrease of the affinity of the receptor towards the second C_{60} unit.

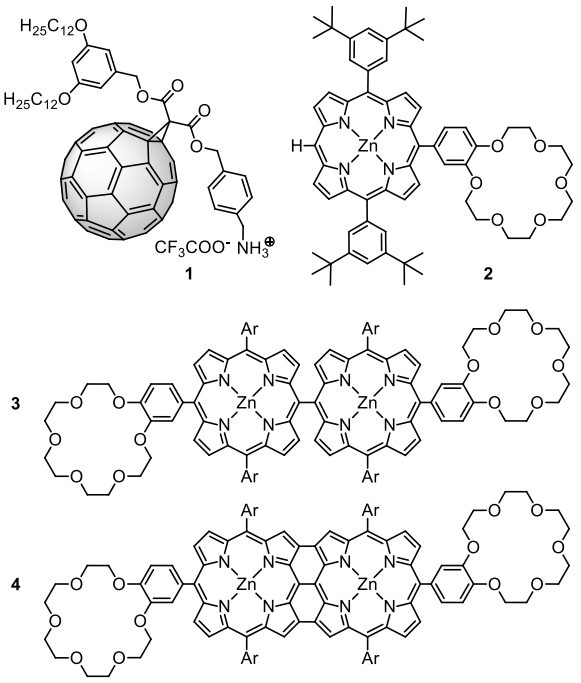

Figure 1. Monoporphyrin **2** was used to obtain host molecules **3** and **4**, which were then complexed with guest molecule **1**.

Herein we report the synthesis of two new ditopic porphyrin receptors for C_{60} (**3** and **4**), appended with crown ether moieties, to study their complexation with the ammonium salt C_{60} derivative **1**[11] (Figure 1). The ammonium-crown ether interaction provides a recognition motif for the supramolecular complexation of two fullerene moieties. While in system **3** the two porphyrins are almost orthogonal, they are fully conjugated in the planar fused compound **4**. Theoretical calculations were carried out to understand the nature of the interactions controlling the association processes with special attention to the cooperative effects experimentally evidenced for these systems. For both porphyrinic receptors, the combination of ammonium-crown-ether interactions with fullerene-porphyrin interactions provided very stable supramolecular ensembles and negative cooperative effects have been evidenced for the binding of the second fullerene-ammonium salt **1**. Actually, the intramolecular C_{60}-porphyrin interactions of the first guest molecule substantially reduce the electron density in the porphyrin dimers **3** and **4** and thus intramolecular interactions of the second fullerene guest with its porphyrinic receptor are less favorable. Interestingly, this effect is however stronger for compound **3** despite the reduced electronic communication between the two porphyrinic moieties when compared to porphyrin tape **4**. Indeed, the negative cooperativity resulting from the fullerene-porphyrin interactions may be partially compensated by additional stabilizing interactions between the guest C_{60} units in the complex formed with **4**.

RESULTS AND DISCUSSION

Synthesis. Porphyrin dimer **3** was obtained by Ag^{I}–promoted oxidative *meso-meso* coupling of monoporphyrin **2**[8a] in $CHCl_3$. The proposed mechanism for this reaction is based on the initial one-electron oxidation of a porphyrin unit by $AgPF_6$, followed by the nucleophilic attack of another neutral porphyrin molecule and its subsequent dehydrogenation.[12] ^{1}H-NMR analysis of the crude reaction mixture after the reaction evidenced the appearance of a signal at −2.92 ppm, corresponding to the partial demetalation of the porphyrin subunits. Therefore, the mixture was treated with a Zn(II) salt to ensure full metalation. Purification of the product was easily achieved by gravity-fed chromatography and gel permeation chromatography due to the good solubility of this derivative, with an orthogonal conformation hampering aggregation by π−π stacking between molecules.

Triply fused porphyrin tape **4** was obtained in an efficient manner using more oxidative conditions, i.e., Sc^{III}-catalyzed oxidation of porphyrin **2** with 2,3-dichloro-5,6-dicyanobenzoquinone. As in the previous case, the reaction was followed by treatment with a Zn(II) salt to ensure full metalation of the product (Scheme S1 in the Supporting Information).

NMR characterization. ^{1}H-NMR spectroscopic analysis of the aromatic region of dimer **3** provided valuable information on its structure. To start with, the characteristic *meso* proton signal of porphyrin **2** at ~10.3 ppm, strongly deshielded by the aromatic ring current, was no longer present (Figures 2a-b). Also, inner pyrrolic protons were shifted upfield by 0.85 ppm, in good agreement with an approximate perpendicular arrangement of both subunits, where the ring current of one porphyrin moiety affects the protons of the other moiety.[12a] Additional through-space correlation NOESY experiments enabled full assignment of all the protons in the aromatic region (Figure S1, Supporting Information).

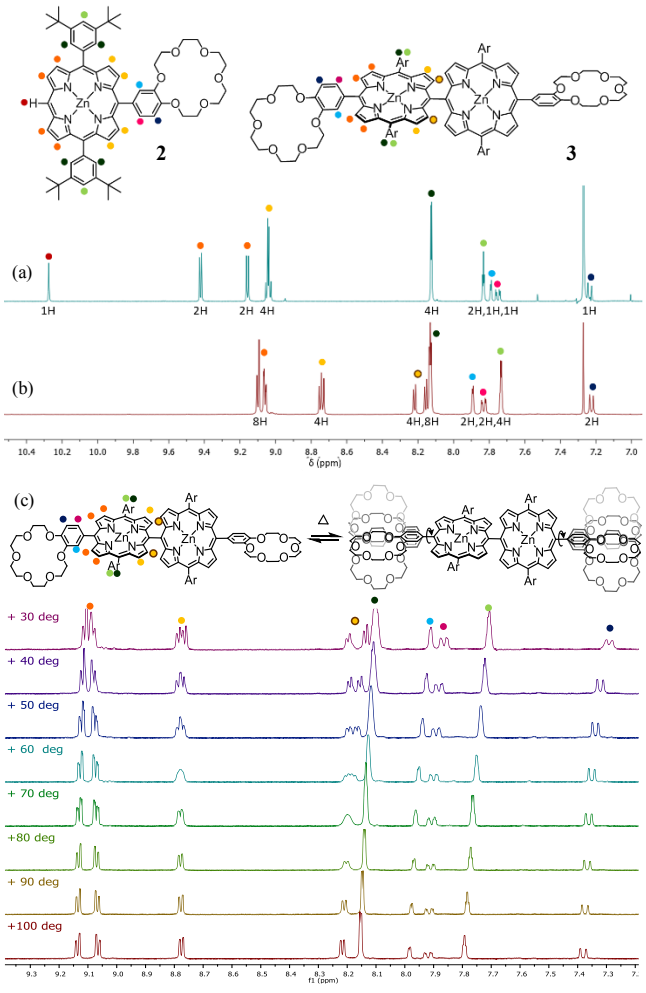

Figure 2. NMR characterization of compound **3**. ^{1}H-NMR ($CDCl_3$, 400 MHz, 298 K) of monoporphyrin **2** (a) versus *meso-meso* dimer **3** (b) and (c) ^{1}H-NMR variable temperature experiments ($ClCD_2CD_2Cl$, 400 MHz, 30-100ºC).

Variable temperature ^{1}H-NMR studies of **3** (Figure 2c) evidenced the presence of a chiral axis across the porphyrin-benzocrown ether bond. Heating the system led to an increase in its kinetic energy, and, thus, the benzocrown ether moieties started to rotate around the porphyrin-phenyl bonds, overcoming their steric hindrance. The rotational barrier was estimated to be *ca.* 17 kcal·mol^{-1} (Figure S2) in line with other experimental measurements on phenyl porphyrins.[13] As a result of the heating, all pyrrolic protons in the porphyrin were then equally affected by the crown ether, changing the apparent symmetry of the system and reducing the complexity of the spectra. This is evidenced by the appearance of two clear AB systems in the pyrrolic region. A similar effect was observed in the signals corresponding to the crown ether moiety (Figure S3). Rotation around the porphyrin-porphyrin bond is not possible at the measurement conditions due to the higher steric hindrance as will be further demonstrated with UV-vis spectra.

NMR characterization was not possible for molecule **4** due to the appearance of very broad signals, probably as a result of the formation of aggregates. However, its characteristic absorption spectrum, together with its MS spectrum, allowed us to unambiguously characterize the product.

UV-vis characterization. The UV-vis absorption spectrum of molecule **3** corresponds to that of a typical *meso-meso* dimer,[11,14] with a large splitting of the Soret band due to exciton coupling and a Q band modestly shifted towards the red in comparison with **2**, suggesting that each of the porphyrin subunits retains its monomeric electronic character.[15] In contrast, dimer **4** exhibits the characteristic absorption spectrum of a triply fused porphyrin tape, with no splitting of the Soret band and the appearance of a low-lying broad band reaching the 1000 nm region (Figure 3).

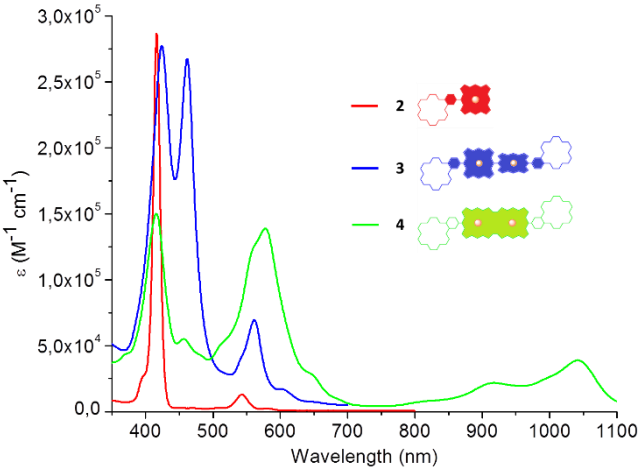

Figure 3. UV-vis spectra of **2** (1.9 ×10^{-6} M, red), **3** (4.7 × 10^{-6} M, blue), and **4** (1.1 × 10^{-5} M, green) in CH_2Cl_2.

Variable temperature absorption measurements (25–95 ^{0}C in PhCl) on porphyrin dimer **3** did not show any clear evidence of rotation around the porphyrin-porphyrin bond (Figure S4).[16]

In order to rationalize the changes observed in the UV-Vis spectra in passing from **2** to **3** and **4**, singlet excited states (S_n) were computed at the B3LYP/(6-31G**+LANL2DZ) level[17] using time-dependent density functional theory (TD-DFT)[18] (see the Supporting Information for full computational details). Table S1 summarizes the most relevant electronic transitions that give shape to the absorption spectra of **2**–**4**. For **2**, the electronic transitions to the two low-lying singlet excited states (S_1 and S_2) are computed about 550 nm. These transitions are weak, with oscillator strengths (*f*) of 0.045 and 0.025, respectively, correspond to electronic excitations locally centered on the porphyrin core, and give rise to the Q band observed experimentally at 548 nm. In addition, states S_5 and S_6 computed around 380 nm are responsible for the Soret band observed at 400 nm. The electronic transitions to S_5 and S_6 possess high oscillator strengths of 1.565 and 0.831, respectively, and also imply electronic excitations mainly located on the porphyrin core (Table S1 and Figure S8).

Moving to the porphyrin *meso-meso* dimer **3**, the electronic transitions to the S_1 and S_2 states associated to the Q band are computed at slightly higher wavelengths (in the 570 nm region) due to the small electronic interaction between the two porphyrin moieties that causes a narrowing of the HOMO−LUMO energy gap from 2.71 eV in **2** to 2.55 eV in **3** (Figure S8 and S10). The Soret band, originating now in the S_{17} state (f = 1.577), is also red-shifted in comparison with **2**. Interestingly, TD-DFT calculations predict an intense S_{11} excited state (f = 1.022) lower in energy than S_{17} and computed at 475 nm, which reproduces the splitting of the Soret band and the peak experimentally observed at 460 nm. This state originates in an electronic excitation of the porphyrin moieties with no implication of the peripheral benzene rings or the crown ether groups.

For porphyrin tape dimer **4**, the two lowest-lying electronic transitions associated with the S_1 and S_2 states are computed in the 960–970 nm range (Table S1). These two moderately-intense transitions (f = 0.312 and 0.089, respectively) originate in porphyrin-centered excitations and give rise to the new broad band observed for **4** in the 800–1100 nm range. Their low energy is due to the complementarity of the two fused porphyrin moieties with an efficient π-conjugation between them, which results in a destabilization/stabilization of the HOMOs/LUMOs and, therefore, in a drastic decrease of the HOMO–LUMO gap (1.55 eV, Figure S10). States S_7 and S_{10} computed in the 520–560 nm range give rise to the typical Q band, which is notoriously more intense than in **2** and **3** as predicted by the oscillator strengths obtained for S_7 (1.150) and S_{10} (0.874). The peripheral benzene rings participate in these states that mainly correspond to the excitation of the porphyrin cores (Table S1 and Figure S9). Finally, several intense transitions are computed in the 385–395 nm region, which give rise to the broad peak observed at 400 nm for the Soret band (Figure 3).

Complexation studies. Supramolecular ensembles were built up by adding increasing quantities of fullerene derivative **1** over the corresponding porphyrin dimers **3** and **4** in CH_2Cl_2 at room temperature (Schemes 1 and 2). Complexation was followed by monitoring the induced UV-visible spectroscopic changes. In the case of dimer **3**, it resulted in a red shift of the Soret bands ($\lambda_{1,max}$ = 422 → 427 nm; $\lambda_{2,max}$ = 458 → 463 nm) evidencing the presence of intermolecular π–π interactions between the host and the guest (Figure 4).[8a] A similar behavior was found for the Soret

band ($\lambda_{1,max}$ = 416 → 426 nm), the Q-band ($\lambda_{2,max}$ = 578 nm → 581 nm), and also the red-shifted absorption bands ($\lambda_{3,max}$ = 917 → 941 nm; $\lambda_{4,max}$ = 1042 → 1063 nm) of porphyrin tape **4** (Figure 5).

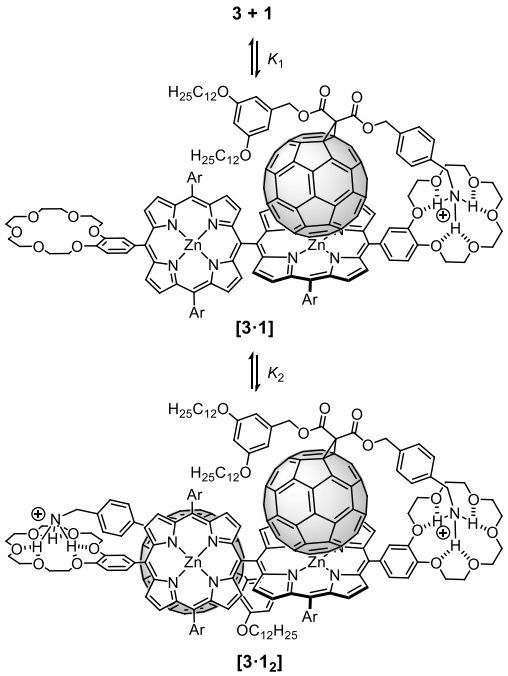

Scheme 1. Supramolecular complexes obtained from building blocks **3** and **1**.

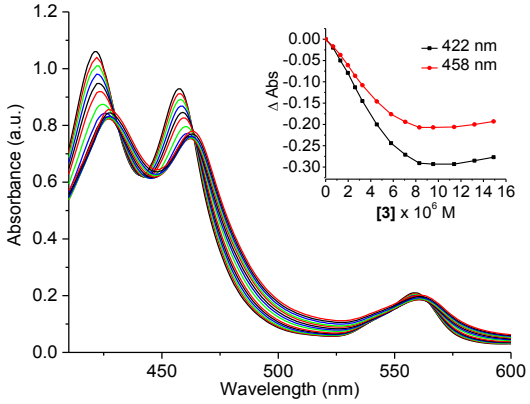

Figure 4. UV-vis spectral changes observed during the complexation of porphyrin dimer **3** (4.72×10^{-6} M) by addition of **1** (0−3.4 equiv) in CH_2Cl_2 at room temperature. Inset shows the binding isotherm of the Soret bands.

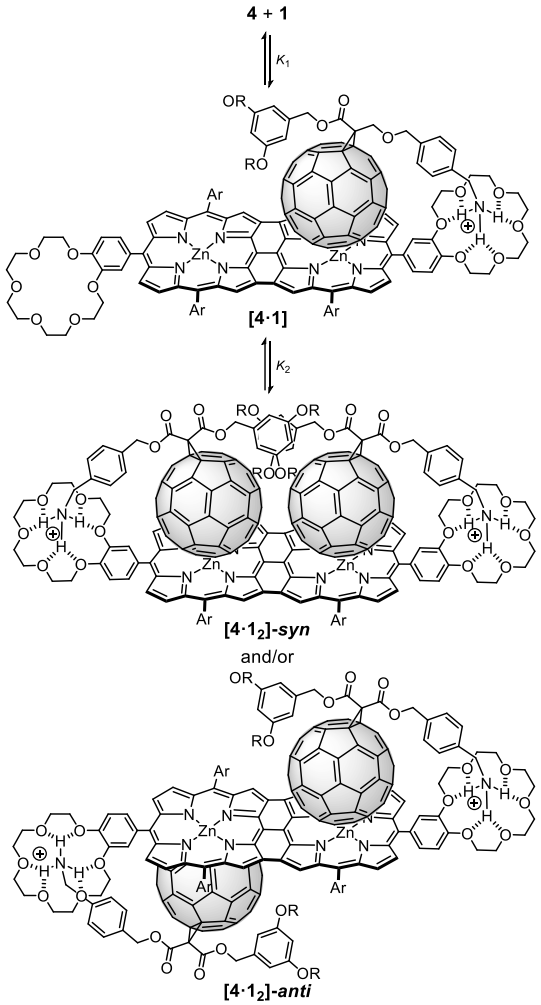

Scheme 2. Supramolecular complexes obtained from building blocks **4** and **1**.

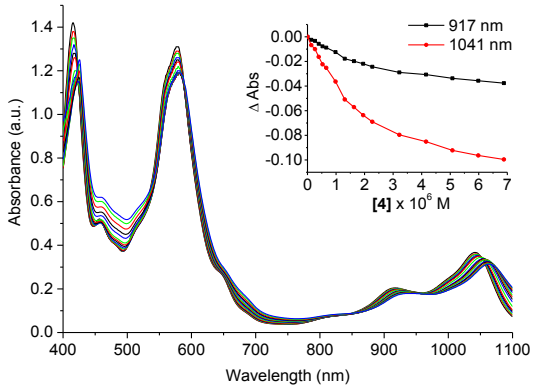

Figure 5. UV-vis spectral changes observed during the complexation of porphyrin tape **4** (1.18×10^{-8} M) by addition of **1** (0−10.5 equiv by 0.7 equiv steps) in CH_2Cl_2 at room temperature. Inset shows the binding isotherm of the low-energy bands.

A 1:2 stoichiometry was foreseen for both **3** and **4** based on the design of the host molecules and the results previously obtained for the analogous monoporphyrin system [**2**·**1**].[8a] This was further corroborated by ESI MS for a 1:2 mixture of porphyrin dimer **3** and methanofullerene **1** in CH_2Cl_2, which exhibited a

double charged ion peak at m/z 2461.0, ascribed to the 1:2 complex after loss of the trifluoroacetate (TFA) counteranions (Figure S5). A similar result was obtained in the ESI-MS analysis of a 1:2 mixture of porphyrin tape **4** and **1** (Figure S6). The peak corresponding to the 1:1 complex was not detected under these conditions in any case, suggesting that 1:2 complexes are the most abundant species in the analyzed solutions.

It is important to note that, in spite of being formed by a myriad of internal micro equilibria leading to semicomplexed species (Scheme S2), the complexation of **3** and **4** by **1** can be simplified in the two-steps processes sketched in Schemes 1 and 2 (see also Scheme S2b). This is possible due to the high effective molarity found for the analogous [**2**·**1**] system (3.16 M^{-1}) evidencing its tendency towards ring-closing under the conditions employed.[8a] Non-linear curve fitting to a 1:2 model yields the association constants (K_a) summarized in Table 1. In the case of the complexes formed with porphyrin tape **4**, curve fitting was better when performed over the region around 750−1100 nm than over the Soret bands region.

Table 1. Stepwise Association Constants for [3·1$_2$] and [4·1$_2$].

log $K_a \pm 3\sigma$		
3	log K_1	8.7 ± 1.4
	log K_2	5.4 ± 0.9
4	log K_1'	6.8 ± 0.5
	log K_2'	5.4 ± 0.3

Analysis of the cooperativity. First evidences of cooperative behavior in the supramolecular complexes formed by **3**−**4** and **1** arise from the shape of the binding isotherms found for both systems, which are not the rectangular hyperbola expected for a non-cooperative system (insets in Figures 4 and 5). Further quantitative analysis can be made if we consider that, even if each of the porphyrin subunits exhibits chelate cooperativity, interactions between subunits can be considered as allosteric (Scheme S2). Therefore, an approximation to the allosteric cooperative factor α can be calculated for these systems.

For **[3·1$_2$]**, α was estimated by eq. 1, where $K \approx K_1$. The value obtained (0.0005) was much lower than unity, thus clearly pointing to a negative cooperativity, i.e., the complexation of the first molecule of **1** leads to a complex where it is more difficult to complex a second equivalent of **1**. This result can be in principle explained by invoking the electronic communication between porphyrin moieties, according to which complexation of a first fullerene molecule by a porphyrin subunit would deplete the electronic density of that porphyrin and its neighbour's, thus decreasing the affinity of the latter towards fullerenes. However, the electronic communication between the porphyrin moieties in **3** is low due to their orthogonal disposition as evidenced above by the UV-vis spectra and the theoretical calculations.

[3·1$_2$] $$\alpha = \frac{K_1 K_2}{K^2} = \frac{K_2}{K_1} = \frac{10^{5.4}}{10^{8.7}} = 0.0005 \qquad (1)$$

The allosteric cooperativity factor obtained for **[4·1$_2$]** (eq. 2) also evidences a negative cooperativity in the system. In this case, a very efficient electronic communication exists between the porphyrin moieties and a significant electronic depletion can be expected for the empty porphyrin unit upon complexation of one fullerene guest.

[4·1$_2$] $$\alpha = \frac{K_2}{K_1} = \frac{10^{5.4}}{10^{6.8}} = 0.04 \qquad (2)$$

Interestingly, the cooperativity factor obtained for **[4·1$_2$]** is 80 times larger than that found for **[3·1$_2$]**, suggesting the existence of other interactions which overcome the electronic depletion of the porphyrin tape upon complexation of the first equivalent of **1**. As depicted in Scheme 2, complex **[4·1$_2$]** can yield two different complexes, **[4·1$_2$]-*syn*** and **[4·1$_2$]-*anti***. Although it is not possible to ascertain which disposition is preferred in solution by spectroscopic measurements, and steric hindrance could be expected to be larger for the *syn* configuration, the possibility of having additional π–π interactions between fullerene moieties in **[4·1$_2$]-*syn***, not existent in **[4·1$_2$]-*anti***, could explain the larger α value obtained, thus pointing to the *syn* disposition as the one preferred in solution. The relative stability of **[4·1$_2$]-*syn*** and **[4·1$_2$]-*anti*** associates is discussed below on the basis of theoretical calculations.

Electrochemical study. The redox potentials of compounds **2–4** and their supramolecular complexes with **1** have been studied by cyclic voltammetry (CV) and Osteryoung square wave voltammetry (OSWV) measurements in CH_2Cl_2 at room temperature. Results are summarized in Table S2 and Figures S11–S16. For compound **2**, two quasireversible one-electron oxidation processes lead to the formation of the corresponding radical-cation, in which an electron is delocalized over the porphyrin, and also to the corresponding dication.

Dimer **3** seems to display a behavior close to that of the corresponding monomer **2** (Table S2 and Figures S11 and S14). Indeed, the two porphyrin rings are poorly conjugated and, as a result, the dimer nearly behaves as the juxtaposition of two monomers. Notwithstanding, some electronic communication exists between the two porphyrin moieties because the first two oxidation waves split in two peaks in passing from **2** to **3**.

In contrast, the conjugation of the two porphyrin units has a huge effect on the redox potentials of tape **4** (Table S2 and Figure S14). Conjugation induces an important lowering of the first oxidation (E^1_{ox} = 0.55 V) and first reduction (E^1_{red} = −0.58 V) potentials as compared to monomer **2** (E^1_{ox} = 0.87 V and E^1_{red} = −1.31 V) and to porphyrin dimer **3** (E^1_{ox} = 0.83 V and E^1_{red} = −1.28 V). This trend is supported by theoretical calculations which predict that the HOMO/LUMO increases/decreases drastically in energy in passing from **2** (−4.73/−2.02 eV) and **3** (−4.63/−2.07 eV) to **4** (−4.31/−2.77 eV). Since the porphyrin rings are efficiently conjugated in tape dimer **4**, the resulting unpaired electron is delocalized over the two rings, giving rise to a completely delocalized π radical cation or anion. Dimer **4** therefore constitutes a single redox entity and the HOMO−LUMO energy gap can be associated with the difference between the first oxidation and first reduction processes: $\Delta' E = E^1_{ox} - E^1_{red}$. Thus, dimer **4** provides a significant decrease in the HOMO–LUMO energy gap as compared to that of monomer **2** ($\Delta' E$(monomer **2**) – $\Delta' E$(tape **4**) = 1.05 V), due to the lowering of the first oxidation potential by 320 mV and of the first reduction potential by 730 mV. The low electrochemical gap is a direct result of the more extended π-conjugation in the planar triply fused system than in the simply fused **3** or monomer **2**. Calculations predict a decrease of 1.16 eV for the HOMO–LUMO energy gap in passing from **2** to **4** in good accord with the value obtained from electrochemical data and literature.[19]

In OSWV, complexation-induced changes are observed in the porphyrin host molecules **2**–**4** upon complexation with guest molecule **1** (see Figures S14-S16)**.** Specifically, a significant decrease of the intensity of the oxidation waves below 1,5 V is detected.

Also, it has been previously observed that porphyrins may influence C_{60} reduction potential, especially its first wave, upon complexation.[2c,8a,11,20] In the particular case of **[4·1$_2$]**, the C_{60} moiety becomes less favorable to reduction upon complexation, as evidenced by a cathodic shift of 60 mV in the first fullerene-centered reduction (Table S2 and Figures S15–S16), thus suggesting an intramolecular fullerene-porphyrin interaction in **[4·1$_2$]**. Even though the first apparent reduction potential of **4** is close to that of the C_{60}, the change observed in Figure S16 after addition of 2 equivalents of C_{60} clearly evidences this interaction: two different peaks at – 0.56 V and – 0.62 V are clearly distinguishable. The magnitude of the potential shift observed for **4** after guest complexation (60 mV) is similar to that found in other supramolecular complexes such as the Zn-porphyrin sandwich designed by Aida and Saigo.[20a] However, these strong shifts are not always present. Indeed, redox potentials of fullerene–donor conjugates are generally very weakly affected by intramolecular π–π interactions, even in cyclic systems in which the two components are forced to be at the van der Waals contact.[2c,21] In our systems, no significant electrochemical changes are detected for **1** upon complexation with **2** and **3** (Table S2).

This difference behavior can be explained on the basis of tape **4** being a better donor molecule than **2** and **3**, with an E^1_{ox} 300 mV lower. This is most likely due to the electronic conjugation across the whole molecule, which may render the donor-acceptor electron transfer to the C_{60} easier, something in full agreement with the calculation of the net electronic charges of the [**3·1**] and [**4·1**] species (see vide infra). Moreover, the analysis of the cooperativity, which emphasizes the role of other interactions, indicates a much higher cooperativity factor for [**4·1$_2$**] than for [**3·1$_2$**].

Computational modeling. Theoretical calculations performed at the DFT B97-D3/(6-31G**+LANL2DZ) level of theory[17b,17c,22] were used to provide deeper understanding of the origin and nature of the intermolecular forces driving the supramolecular assembly of dimers **3** and **4** with the fullerene-based compound **1** (see the SI for computational details).

In **[3·1]**, compound **1** interacts with the crown ether through the positively charged ammonium group forming three N–H···O(ether) hydrogen-bond interactions in the 1.83–2.00 Å range (Figure 6a). This interaction has been recently demonstrated to be the promoting force in the supramolecular assembly between guest **1** and related metalloporphyrin-based hosts with a net stabilizing energy that amounts to –64.9 kcal/mol.[8a] The fullerene ball of **1** favorably interacts with the porphyrin core of **3** with short metal···C(C_{60}) contacts of 3.14 Å. This interaction originates not only from dispersion forces arising from long-range electron correlation effects but also from strong electrostatic effects when considering metal-substituted porphyrins.[8a] Furthermore, short H···C contacts between the peripheral *tert*-butyl-substituted phenyl rings and C_{60} are computed in the range of 2.5–3.2 Å, which add approximately 1 kcal/mol per each interaction to the final stabilization energy of the complex. More importantly, the vicinal porphyrin, linked to the porphyrin that interacts with **1**, approaches the fullerene fragment and gives rise to additional interactions: short H···C contacts in the 2.7–3.2 Å range and a weak π–π interaction between the peripheral benzene ring and the fullerene. In fact, the empty porphyrin core is distorted from linearity with respect to the occupied porphyrin core by approximately 8° to maximize the interaction with C_{60} (Figure 6a). These additional interactions, which are not present in [**2·1**], can be a plausible explanation for the higher experimental association constant found for porphyrin dimer **3** (log K_1 = 8.7 ± 1.4) in comparison with monoporphyrin **2** (log K_a = 6.9 ± 0.2).[8a]

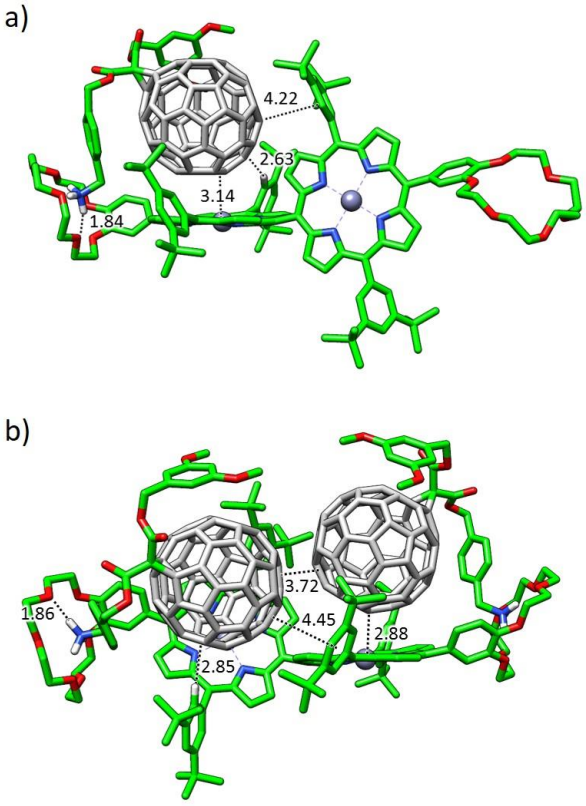

Figure 6. Minimum-energy geometry computed for supramolecular complexes **[3·1]** (a) and **[3·1$_2$]** (b) at the B97-D3/(6-31G**+LANL2DZ) level of theory. Selected intermolecular distances are given in Å. Hydrogen atoms are omitted for clarity.

Moving to **[3·1$_2$]**, the second molecule of **1** enters the empty porphyrin core and defines similar interactions to those described for **[3·1]**. The minimum-energy geometry shows that the two fullerenes tend to approximate each other in order to stabilize the resulting complex (Figure 6b). Close C···C contacts between the two C_{60} are computed at 3.7 Å. Again, the peripheral di-*tert*-butylphenyl groups placed on the vicinal porphyrin moieties play an active role in the stabilization of the complex with short H···C(C_{60}) contacts around 2.8 Å and π–π interactions at 4.4 Å.

The association between porphyrin tape **4** and **1** (Figure 7a) follows the same pattern as previously described for **[3·1]**. The ammonium group is bound to the crown ether forming efficient short N–H···O(ether) contacts in the 1.94–1.97 Å range. The fullerene interacts with the porphyrin core and with the di-*tert*-butylphenyl groups through metal···C_{60} contacts of 2.87 Å and H···C_{60} distances in the range of 2.7–3.1 Å, respectively. Oddly, the dimer porphyrin tape becomes curved to better embrace the fullerene ball and further stabilize the complex. In contrast to that previously described in [**3·1**], the di-*tert*-butylphenyl groups of the vicinal porphyrin core are not close enough to interact with C_{60} (closest H···C(C_{60}) contact calculated at 3.80 Å) and, there-

fore, they do not contribute in the stabilization of the **[4·1]** complex (Figure 7a).

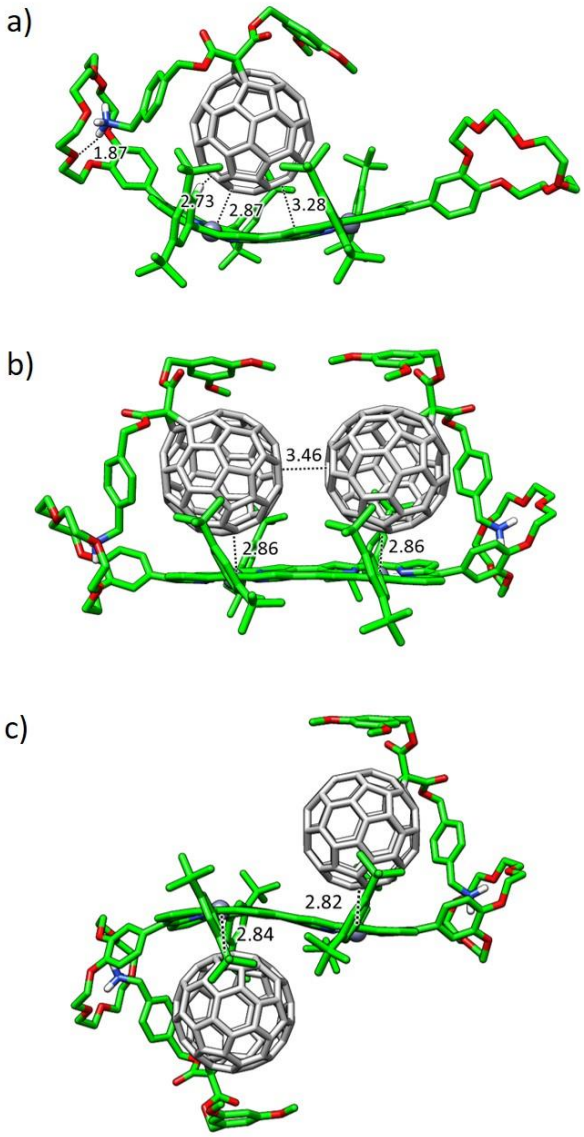

Figure 7. Minimum-energy geometry computed for **[4·1]** (a) **[4·1$_2$]-*syn*** (b) and **[4·1$_2$]-*trans*** (c) at the B97-D3/(6-31G**+LANL2DZ) level of theory. Selected intermolecular distances are given in Å. Hydrogen atoms are omitted for clarity.

The introduction of the second fullerene-based guest **1** into the **[4·1]** complex can be achieved in two different ways: the two fullerene balls standing in the same side in a *syn* disposition (**[4·1$_2$]-*syn***), or the two balls located in opposite sides with respect to the plane generated by the porphyrin tape dimer in an *anti* disposition (**[4·1$_2$]-*anti***) (Figure 7b and c). In both cases, all the previous intermolecular interactions described for **[4·1]** exist in the stoichiometric complex 1:2 with short metal···C_{60} contacts in the range of 2.82–2.99 Å and di-*tert*-butylphenyl–C_{60} H···C contacts of 2.7–3.1 Å. However, by comparing the *anti* with the *syn* complexes, an important π–π stabilizing interaction arises for the latter due to the fullerene-fullerene proximity (ring-to-ring distance calculated at 3.46 Å). A recent study on related fullerene-based adducts showed the key importance of the stabilizing C_{60}–C_{60} interactions, resulting in an energy differentiation between the *syn* and *anti* dispositions of more than 5 kcal/mol in favor of *syn*.[23]

Single-point energy B97-D3 calculations were performed on the B97-D3/(6-31G**+LANL2DZ)-optimized geometries by using the more extended cc-pVTZ+LANL2DZ basis set to estimate the binding energy (E_{bind}) for all the supramolecular complexes (Table 2). The association of one molecule of **1** to the *meso-meso* porphyrin dimer **3** leads to a large net stabilization of –108.19 kcal/mol rising especially from the N–H···O(ether) contacts and the porphyrin core–C_{60} interaction. Additionally, the di-*tert*-butylphenyl groups contribute to the final stabilization of the complex by approximately 1 kcal/mol per H···C_{60} contact (total number of contacts = 6). Upon the inclusion of the second molecule of **1**, E_{bind} is approximately doubled, reaching a value of –211.05 kcal/mol for **[3·1$_2$]**. The additional fullerene-fullerene stabilizing interactions in **[3·1$_2$]** with respect to **[3·1]** are counteracted by the poorer disposition of the balls to interact with the di-*tert*-butylphenyl groups of the vicinal porphyrin moiety that contribute to the stabilization of **[3·1]**.

Table 2. Binding Energies Computed at the B97-D3/(cc-pVTZ+LANL2DZ) Level for the Host-Guest Supramolecular Associates with Stoichiometry 1:1 and 1:2.

Complex	E_{bind} (kcal/mol)
[3·1]	–108.19
[3·1$_2$]	–211.05
[4·1]	–98.40
[4·1$_2$]-*anti*	–195.46
[4·1$_2$]-*syn*	–200.20

For **[4·1]**, the binding energy is computed to be –98.40 kcal/mol. This value is 10 kcal/mol lower than in **[3·1]** due to the less-efficient interaction with the vicinal empty porphyrin (compare Figures 6a and 7a). Upon addition of the second molecule of **1** in an *anti* disposition (**[4·1$_2$]-*anti***), E_{bind} is computed at –195.46 kcal/mol, almost twice the binding energy of **[4·1]** (Table 2). Finally, a slightly larger stabilization of –200.20 kcal/mol is obtained for the **[4·1$_2$-*syn*]** complex. As suggested above, the additional C_{60}–C_{60} interaction with a short π–π contact calculated at 3.46 Å overcomes the steric hindrance between the two balls and makes the *syn* complex 5 kcal/mol more stable than the *anti*. This value is in good accord with the energy difference of 6.36 kcal/mol recently reported in favor of the *cis* configuration in a related pentacene-C_{60} derivative.[23]

The theoretical values predicted for E_{bind} (Table 2) therefore indicate that the incorporation of the first guest molecule leads to a more stable complex for **3** than for **4**, and suggest that the entrance of the second molecule of **1** is more favored for **4** than for **3**. These trends are in accord with the higher association constant $K1$ obtained for **3** compared to **4** and with the smaller decrease it experiences for **4** in passing from the 1:1 to the 1:2 stoichiometry (Table 1). A direct correlation between the theoretical values predicted for E_{bind} and the experimental values of K_a is however not straightforward because calculations do not take into account the desolvation energy needed to form the complexes in solution.

To help in the rationalization of the experimental values of the association constants for both the 1:1 and 1:2 complexes (Table 1), net electronic charges were calculated at the B97-D3/(6-31G**+LANL2DZ) level for **[3·1]** and **[4·1]** using the natural population analysis (NPA) approach.[24] Upon inclusion of the first **1** molecule, the electron-donor porphyrin dimer **3** transfers 0.19e to the fullerene-based acceptor. The porphyrin moiety interacting with the C_{60} ball accumulates a positive charge of +0.16e whereas the vicinal empty porphyrin bears a residual positive charge of only +0.03e. Moving to **[4·1]**, the fullerene-based **1** system borrows 0.26e from the porphyrin dimer. In contrast to **[3·1]**, the C_{60}-interacting porphyrin moiety bears a smaller positive charge of +0.11e compared to the empty porphyrin fragment (+0.15e). The efficient π-conjugation between the two porphyrin moieties in tape porphyrin **4** explains the charge transfer from one fragment to the other. Theoretical calculations therefore predict a notable decrease in the electron density for both *meso* and tape porphyrin dimers in the ground state upon complexation of the first **1** acceptor molecule. The decrease of electronic density disfavors the entrance of the second guest molecule and contributes to the remarkable change of the association constant (log K_a) from 8.7 to 5.4 in **[3·1$_2$]**, and from 6.8 to 5.4 in **[4·1$_2$]**, when the second **1** molecule is included to form the stoichiometric 1:2 complex. For complex **[4·1$_2$]**, the stabilizing interactions between the C_{60} units found for the more stable *cis* disposition partially compensates for the negative effect provoked by the lowered electronic density. However, other factors such as the steric hindrance provoked by the long alkyl chains born by the guest molecules should be considered to fully justify these trends and the higher negative cooperativity shown by **3** compared to **4**.

CONCLUSION

In conclusion, we have studied the supramolecular interaction of porphyrin dimer **3** and porphyrin tape **4**, endowed with crown ether rings, with C_{60} derivative **1**. The formation of the complexes is driven by the complementary ammonium-crown ether H-bonding interactions and the π–π interactions between the porphyrin rings and the C_{60} moieties. Both porphyrin systems form complexes with 1:1 and 1:2 stoichiometries, and present a negative cooperativity, showing a decrease of the binding constants for the complexation of the second fullerene unit. This fact is justified by the decrease of the donating ability of the second porphyrin moiety once the first fullerene unit has been added. In the case of compound **4**, the two porphyrins moieties present a very effective π-conjugation that allows for a larger charge transfer between them upon the inclusion of the first guest molecule. However, this negative effect is partially compensated by the favorable π–π interaction between the two fullerene guests in the more stable *syn* disposition of **[4·1$_2$]** and, therefore, the decrease of the binding constant for the addition of the second fullerene unit in **[4·1$_2$]** is not as large as observed for **[3·1$_2$]**. The supramolecular arrays studied in this work constitute singular examples that will help one to better understand the supramolecular recognition of fullerenes by porphyrin-based hosts, in the quest for efficient charge- and energy-transfer architectures potentially useful in artificial photosynthesis and organic photovoltaics.

ASSOCIATED CONTENT

Supporting Information. Experimental and computation details. Figures S1–S16. Tables S1–S2. Schemes S1–S2. This material is available free of charge via the Internet at http://pubs.acs.org.

AUTHOR INFORMATION

Corresponding Author

enrique.orti@uv.es
nazmar@ucm.es
nierengarten@unistra.fr

ACKNOWLEDGMENT

Financial support by the European Research Council (ERC-320441-Chiralcarbon), the Ministerio de Economía y Competitividad (MINECO) of Spain (projects CTQ2014-52045-R, CTQ2015-71154-P and Unidad de Excelencia María de Maeztu MDM-2015-0538), the Comunidad Autónoma de Madrid (PHOTOCARBON project S2013/MIT-2841), the Generalitat Valenciana (PROMETEO/2016/135), European FEDER funds (CTQ2015-71154-P), the International Center for Frontier Research in Chemistry (icFRC) and the Labex Chimie des Systèmes Complexes is acknowledged. L.M. thanks the Obra Social "la Caixa" for a postgraduate fellowship. J.C. acknowledges the Spanish Ministry of Education, Culture, and Sport (MECD) for a FPU grant. N.M. thanks to Alexander von Humboldt Foundation.

REFERENCES

(1) a) Garg, V.; Kodis, G.; Chachisvilis, M.; Hambourger, M.; Moore, A. L.; Moore, T. A.; Gust, D. *J. Am. Chem. Soc.* **2011**, *133*, 2944; b) Guldi, D. M. *Chem. Soc. Rev.* **2002**, *31*, 22; c) Kuramochi, Y.; Sandanayaka, A. S. D.; Satake, A.; Araki, Y.; Ogawa, K.; Ito, O.; Kobuke, Y. *Chem. Eur. J.* **2009**, *15*, 2317; d) Kuhri, S.; Charalambidis, G.; Angaridis, P. A.; Lazarides, T.; Pagona, G.; Tagmatarchis, N.; Coutsolelos, A. G.; Guldi, D. M. *Chem. Eur. J.* **2014**, *20*, 2049; e) Umeyama, T.; Imahori, H. *Photosynth. Res.* **2006**, *87*, 63; f) Wielopolski, M.; Molina-Ontoria, A.; Schubert, C.; Margraf, J. T.; Krokos, E.; Kirschner, J.; Gouloumis, A.; Clark, T.; Guldi, D. M.; Martín, N. *J. Am. Chem. Soc.* **2013**, *135*, 10372; g) Fukuzumi, S.; Ohkubo, K.; D'Souza, F.; Sessler, J. L. *Chem. Commun.* **2012**, *48*, 9801.

(2) a) Boyd, P. D. W.; Hodgson, M. C.; Rickard, C. E. F.; Oliver, A. G.; Chaker, L.; Brothers, P. J.; Bolskar, R. D.; Tham, F. S.; Reed, C. A. *J. Am. Chem. Soc.* **1999**, *121*, 10487; b) Kimura, M.; Saito, Y.; Ohta, K.; Hanabusa, K.; Shirai, H.; Kobayashi, N. *J. Am. Chem. Soc.* **2002**, *124*, 5274; c) Saegusa, Y.; Ishizuka, T.; Kojima, T.; Mori, S.; Kawano, M.; Kojima, T. *Chem. Eur. J.* **2015**, *21*, 5302.

(3) a) Hosseini, A.; Taylor, S.; Accorsi, G.; Armaroli, N.; Reed, C. A.; Boyd, P. D. W. *J. Am. Chem. Soc.* **2006**, *128*, 15903; b) Durot, S.; Taesch, J.; Heitz, V. *Chem. Rev.* **2014**, *114*, 8542; c) Garcia-Simon, C.; Costas, M.; Ribas, X. *Chem. Soc. Rev.* **2016**, *45*, 40; d) Nakamura, T.; Ube, H.; Miyake, R.; Shionoya, M. *J. Am. Chem. Soc.* **2013**, *135*, 18790; e) Song, J.; Aratani, N.; Shinokubo, H.; Osuka, A. *J. Am. Chem. Soc.* **2010**, *132*, 16356; f) Meng, W.; Breiner, B.; Rissanen, K.; Thoburn, J. D.; Clegg, J. K.; Nitschke, J. R. *Angew. Chem. Int. Ed.* **2011**, *50*, 3479.

(4) a) Stangel, C.; Schubert, C.; Kuhri, S.; Rotas, G.; Margraf, J. T.; Regulska, E.; Clark, T.; Torres, T.; Tagmatarchis, N.; Coutsolelos, A. G.; Guldi, D. M. *Nanoscale* **2015**, *7*, 2597; b) Garg, V.; Kodis, G.; Liddell, P. A.; Terazono, Y.; Moore, T. A.; Moore, A. L.; Gust, D. *J. Phys. Chem. B* **2013**, *117*, 11299; c) D'Souza, F.; Smith, P. M.; Zandler, M. E.; McCarty, A. L.; Itou, M.; Araki, Y.; Ito, O. *J. Am. Chem. Soc.* **2004**, *126*, 7898; d) Trabolsi, A.; Elhabiri, M.; Urbani, M.; Delgado de la Cruz, J. L.; Ajamaa, F.; Solladie, N.; Albrecht-Gary, A.-M.; Nierengarten, J.-F. *Chem. Commun.* **2005**, 5736; e) Lee, C. Y.; Jang, J. K.; Kim, C. H.; Jung, J.; Park, B. K.; Park, J.; Choi, W.; Han, Y.-K.; Joo, T.; Park, J. T. *Chem. Eur. J.* **2010**, *16*, 5586.

(5) a) Dordevic, L.; Marangoni, T.; De Leo, F.; Papagiannouli, I.; Aloukos, P.; Couris, S.; Pavoni, E.; Monti, F.; Armaroli, N.; Prato, M.; Bonifazi, D. *Phys. Chem. Chem. Phys.* **2016**, *18*, 11858; b) Xenogiannopoulou, E.; Medved, M.; Iliopoulos, K.; Couris, S.; Papadopoulos, M. G.; Bonifazi, D.; Sooambar, C.; Mateo-Alonso, A.; Prato, M. *ChemPhysChem* **2007**, *8*, 1056; c) Aloukos, P.; Iliopoulos, K.; Couris, S.; Guldi, D. M.; Sooambar, C.; Mateo-Alonso, A.; Nagaswaran, P. G.; Bonifazi, D.; Prato, M. *J. Mater. Chem.* **2011**, *21*, 2524; d) Sánchez,

L.; Sierra, M.; Martín, N.; Myles, A. J.; Dale, T. J.; Rebek, J.; Seitz, W.; Guldi, D. M. *Angew. Chem. Int. Ed.* **2006**, *45*, 4637; e) Wessendorf, F.; Grimm, B.; Guldi, D. M.; Hirsch, A. *J. Am. Chem. Soc.* **2010**, *132*, 10786; f) Maligaspe, E.; Tkachenko, N. V.; Subbaiyan, N. K.; Chitta, R.; Zandler, M. E.; Lemmetyinen, H.; D'Souza, F. *J. Phys. Chem. A* **2009**, *113*, 8478; g) D'Souza, F.; Wijesinghe, C. A.; El-Khouly, M. E.; Hudson, J.; Niemi, M.; Lemmetyinen, H.; Tkachenko, N. V.; Zandler, M. E.; Fukuzumi, S. *Phys. Chem. Chem. Phys.* **2011**, *13*, 18168; h) D'Souza, F.; Venukadasula, G. M.; Yamanaka, K.-i.; Subbaiyan, N. K.; Zandler, M. E.; Ito, O. *Org. Biomol. Chem.* **2009**, *7*, 1076; i) Wessendorf, F.; Gnichwitz, J.-F.; Sarova, G. H.; Hager, K.; Hartnagel, U.; Guldi, D. M.; Hirsch, A. *J. Am. Chem. Soc.* **2007**, *129*, 16057; j) D'Souza, F.; Maligaspe, E.; Ohkubo, K.; Zandler, M. E.; Subbaiyan, N. K.; Fukuzumi, S. *J. Am. Chem. Soc.* **2009**, *131*, 8787.
(6) a) Balbinot, D.; Atalick, S.; Guldi, D. M.; Hatzimarinaki, M.; Hirsch, A.; Jux, N. *J. Phys. Chem. B* **2003**, *107*, 13273; b) Grimm, B.; Karnas, E.; Brettreich, M.; Ohta, K.; Hirsch, A.; Guldi, D. M.; Torres, T.; Sessler, J. L. *J. Phys. Chem. B* **2010**, *114*, 14134.
(7) a) Megiatto, J. D.; Schuster, D. I.; de Miguel, G.; Wolfrum, S.; Guldi, D. M. *Chem. Mater.* **2012**, *24*, 2472; b) Megiatto, J. D.; Schuster, D. I.; Abwandner, S.; de Miguel, G.; Guldi, D. M. *J. Am. Chem. Soc.* **2010**, *132*, 3847; c) Jakob, M.; Berg, A.; Rubin, R.; Levanon, H.; Li, K.; Schuster, D. I. *J. Phys. Chem. A* **2009**, *113*, 5846; d) Megiatto, J. D.; Li, K.; Schuster, D. I.; Palkar, A.; Herranz, M. Á.; Echegoyen, L.; Abwandner, S.; de Miguel, G.; Guldi, D. M. *J. Phys. Chem. B* **2010**, *114*, 14408; e) Sasabe, H.; Sandanayaka, A. S. D.; Kihara, N.; Furusho, Y.; Takata, T.; Araki, Y.; Ito, O. *Phys. Chem. Chem. Phys.* **2009**, *11*, 10908; f) Li, K.; Schuster, D. I.; Guldi, D. M.; Herranz, M. Á.; Echegoyen, L. *J. Am. Chem. Soc.* **2004**, *126*, 3388; g) Watanabe, N.; Kihara, N.; Furusho, Y.; Takata, T.; Araki, Y.; Ito, O. *Angew. Chem. Int. Ed.* **2003**, *42*, 681.
(8) a) Moreira, L.; Calbo, J.; Illescas, B. M.; Aragó, J.; Nierengarten, I.; Delavaux-Nicot, B.; Ortí, E.; Martín, N.; Nierengarten, J.-F. *Angew. Chem. Int. Ed.* **2015**, *54*, 1255; b) Calderon, R. M. K.; Valero, J.; Grimm, B.; de Mendoza, J.; Guldi, D. M. *J. Am. Chem. Soc.* **2014**, *136*, 11436; c) Wu, Z.-Q.; Shao, X.-B.; Li, C.; Hou, J.-L.; Wang, K.; Jiang, X.-K.; Li, Z.-T. *J. Am. Chem. Soc.* **2005**, *127*, 17460; d) Solladie, N.; Walther, M. E.; Gross, M.; Figueira Duarte, T. M.; Bourgogne, C.; Nierengarten, J.-F. *Chem. Commun.* **2003**, 2412; e) D'Souza, F.; Chitta, R.; Gadde, S.; Zandler, M. E.; McCarty, A. L.; Sandanayaka, A. S. D.; Araki, Y.; Ito, O. *J. Phys. Chem. A* **2006**, *110*, 4338; f) Fang, X.; Zhu, Y.-Z.; Zheng, J.-Y. *J. Org. Chem.* **2014**, *79*, 1184.
(9) Trabolsi, A.; Urbani, M.; Delgado, J. L.; Ajamaa, F.; Elhabiri, M.; Solladié, N.; Nierengarten, J.-F.; Albrecht-Gary, A.-M. *New J. Chem.* **2008**, *32*, 159.
(10) Sato, H.; Tashiro, K.; Shinmori, H.; Osuka, A.; Murata, Y.; Komatsu, K.; Aida, T. *J. Am. Chem. Soc.* **2005**, *127*, 13086.
(11) Bonifazi, D.; Accorsi, G.; Armaroli, N.; Song, F.; Palkar, A.; Echegoyen, L.; Scholl, M.; Seiler, P.; Jaun, B.; Diederich, F. *Helv. Chim. Acta* **2005**, *88*, 1839.
(12) a) Osuka, A.; Shimidzu, H. *Angew. Chem. Int. Ed.* **1997**, *36*, 135; b) Ogawa, T.; Nishimoto, Y.; Yoshida, N.; Ono, N.; Osuka, A. *Angew. Chem. Int. Ed.* **1999**, *38*, 176.
(13) Medforth, C. J.; Haddad, R. E.; Muzzi, C. M.; Dooley, N. R.; Jaquinod, L.; Shyr, D. C.; Nurco, D. J.; Olmstead, M. M.; Smith, K. M.; Ma, J.-G.; Shelnutt, J. A. *Inorg. Chem.* **2003**, *42*, 2227.
(14) Cho, H. S.; Jeong, D. H.; Cho, S.; Kim, D.; Matsuzaki, Y.; Tanaka, K.; Tsuda, A.; Osuka, A. *J. Am. Chem. Soc.* **2002**, *124*, 14642.
(15) Kim, Y. H.; Jeong, D. H.; Kim, D.; Jeoung, S. C.; Cho, H. S.; Kim, S. K.; Aratani, N.; Osuka, A. *J. Am. Chem. Soc.* **2001**, *123*, 76.
(16) Kim, D.; Osuka, A. *J. Phys. Chem. A* **2003**, *107*, 8791.
(17) a) Becke, A. D. *J. Chem. Phys.* **1993**, *98*, 5648; b) Francl, M. M.; Pietro, W. J.; Hehre, W. J.; Binkley, J. S.; Gordon, M. S.; DeFrees, D. J.; Pople, J. A. *J. Chem. Phys.* **1982**, *77*, 3654; c) Hay, P. J.; Wadt, W. R. *J. Chem. Phys.* **1985**, *82*, 299.
(18) Casida, M. E.; Jamorski, C.; Casida, K. C.; Salahub, D. R. *J. Chem. Phys.* **1998**, *108*, 4439.
(19) Fendt, L.-A.; Fang, H.; Plonska-Brzezinska, M. E.; Zhang, S.; Cheng, F.; Braun, C.; Echegoyen, L.; Diederich, F. *Eur. J. Org. Chem.* **2007**, *2007*, 4659.
(20) a) Tashiro, K.; Aida, T.; Zheng, J.-Y.; Kinbara, K.; Saigo, K.; Sakamoto, S.; Yamaguchi, K. *J. Am. Chem. Soc.* **1999**, *121*, 9477; b) Sutton, L. R.; Scheloske, M.; Pirner, K. S.; Hirsch, A.; Guldi, D. M.; Gisselbrecht, J.-P. *J. Am. Chem. Soc.* **2004**, *126*, 10370.
(21) a) Bourgeois, J.-P.; Diederich, F.; Echegoyen, L.; Nierengarten, J.-F. *Helv. Chim. Acta* **1998**, *81*, 1835; b) Figueira-Duarte, T. M.; Lloveras, V.; Vidal-Gancedo, J.; Delavaux-Nicot, B.; Duhayon, C.; Veciana, J.; Rovira, C.; Nierengarten, J.-F. *Eur. J. Org. Chem.* **2009**, *2009*, 5779; c) Mukherjee, S.; Banerjee, S.; Bauri, A. K.; Bhattacharya, S. *J. Mol. Struct.* **2011**, *1004*, 13; d) Iehl, J.; Vartanian, M.; Holler, M.; Nierengarten, J.-F.; Delavaux-Nicot, B.; Strub, J.-M.; Van Dorsselaer, A.; Wu, Y.; Mohanraj, J.; Yoosaf, K.; Armaroli, N. *J. Mater. Chem.* **2011**, *21*, 1562.
(22) a) Grimme, S.; Antony, J.; Ehrlich, S.; Krieg, H. *J. Chem. Phys.* **2010**, *132*, 154104; b) Grimme, S.; Ehrlich, S.; Goerigk, L. *J. Comput. Chem.* **2011**, *32*, 1456.
(23) Zhang, J.; Dolg, M. *Chem. Eur. J.* **2014**, *20*, 13909.
(24) Reed, A. E.; Weinstock, R. B.; Weinhold, F. *J. Chem. Phys.* **1985**, *83*, 735.

For Table of Contents only